# A Chemical Strategy for the Cell-Based Detection of HDAC Activity

Himashinie V. K. Diyabalanage, Genevieve C. Van de Bittner, Emily L. Ricq, and Jacob M. Hooker*

Athinoula A. Martinos Center for Biomedical Imaging, Department of Radiology, Massachusetts General Hospital, Harvard Medical School, Charlestown, Massachusetts 02129, United States

S Supporting Information

ABSTRACT: A strategy for activity-based enzyme detection using a novel enamide-based chemical strategy is described. Enzymatic cleavage of an amide bond results in the formation of an aldehyde. The interaction of this aldehyde with proteins increases retention in cells that express the enzyme. Proof of concept for this enamide-based strategy is demonstrated by detecting histone deacetylase (HDAC) activity in HeLa cells. The modular design of this strategy makes it amenable to *in vitro* and *in vivo* detection.
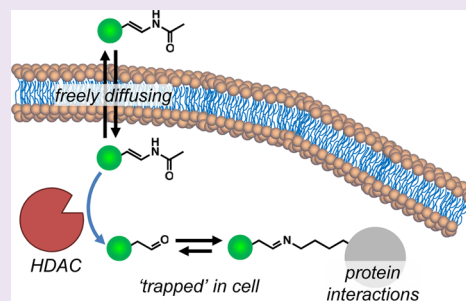
Enzymatic modification of small molecule imaging probes is used to detect changes in enzyme expression or activation within cells, tissues, or organisms.[1−5] Although activity-based enzyme probes are widely used for *in vitro* and cellular studies, translation to *in vivo* imaging studies can be limited when the probe design lacks a method for cellular or tissue retention following interaction with an enzyme target.[5−12] Localization to the site of enzyme activity can be achieved by designing the probe's pharmacokinetic properties to change following enzymatic modification, trapping the probe within the cell, as is the case with ^{18}F-fluorodeoxyglucose (FDG) imaging.[13,14] Using a novel pharmacokinetic alteration strategy, we designed a method to localize activity-based imaging probes to the vicinity of the enzyme of interest, thus increasing intracellular accumulation in cells with higher enzymatic activity. Specifically, (i) an enamide is enzymatically cleaved at the amide bond, (ii) an aldehyde is formed via tautomerization and hydrolysis of the released enamine intermediate, and (iii) the aldehyde is retained within the cell due to nonspecific interaction with nucleophiles (e.g., lysine residues of proteins) within the cell (Figure 1).
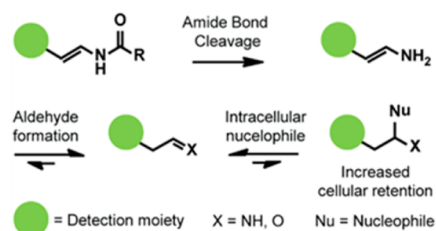

Figure 1. Cell-localized, activity-based enzyme detection. Cleavage of the amide bond of the enamide followed by conversion to aldehyde leads to increased cellular retention due to reaction with adventitious intracellular nucleophiles.

In addition to providing a mechanism for intracellular trapping, this enamide strategy transcends the limitations of many *in vitro* imaging strategies, as its modular design makes it suitable for labeling with magnetic resonance imaging contrast agents or radioisotopes for positron emission tomography.[15] Furthermore, this method affords a potential strategy for focused drug accumulation of therapeutics in cellular subpopulations expressing specific enzymes. From a synthetic standpoint, the enamide functionality also offers the potential for use as a unique, aldehyde-specific protecting group, akin to a silyl enolether. The use of an enamide functional group in these and other synthesic strategies has not, to the best of our knowledge, been explored.

In the present report, we have demonstrated preliminary support for our enamide strategy through reaction with and detection of the activity of a specific class of enzymes, the histone deacetylases (HDACs).[16] HDACs regulate the level of ε-amino acetylation of histone lysine residues, thereby controlling transcriptional regulation via chromatin remodeling.[16−20] Published reports indicate that irregular transcription resulting from altered expression levels of HDACs is associated with cancer, neurodegenerative diseases, and psychiatric conditions, making HDACs important drug targets for these diseases.[21−30] To detect HDAC deacetylation, we used an enamide bearing an *N*-acetyl group, which forms an aldehyde following deacetylation, thus leading to intracellular accumulation (Figure 1). Existing HDAC activity-based probes require UV light-induced photo-cross-linking for enzyme localization, which is incompatible for *in vivo* studies.[31,32] A fluorescent probe, HDAC Probe-1 (HP-1), was designed for proof of concept studies aimed at demonstrating HDAC-specific intracellular accumulation. HP-1 is a derivative of 7-nitro-

Scheme 1. Synthesis of HP-1 Is Achieved in 9 Steps and Enzymatic Deacetylation of HP-1 Forms DHP-1
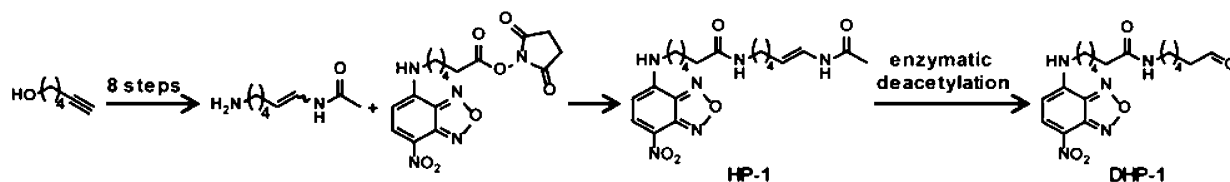
benzo-2-oxa-1,3-diazole (NBD) that bears an aliphatic linker, akin to a lysine side chain, with a terminal enamide (Scheme 1 and Supplementary Scheme S1). During the synthesis of HP-1, we found the *trans* and *cis* isomers to be nonisolable, with the isomers consistently obtained in a 1.5:1 *trans:cis* mixture. Therefore, all experiments were completed using this isomeric mixture. In addition to HP-1, we synthesized HDAC probe-2 (HP-2, Supplementary Scheme S2), which lacks the double bond present in HP-1 and therefore cannot tautomerize to an aldehyde. Comparison of HP-1 and -2 was used to determine the impact of the double bond on deacetylation selectivity among HDAC isoforms and the necessity of aldehyde formation for intracellular retention of deacetylated HP-1 (DHP-1).

Our first studies involved analyzing the stability of the enamide functionality by incubating model compound **9** (Supplementary Figure S1) in HDAC assay buffer at pH 2−12 for 60 min. The solutions were analyzed by HPLC at various time points during the incubation to determine the amount of conversion to the corresponding aldehyde (Supplementary Figure S1). At pH 4−12, there was no detectable conversion to the aldehyde after 60 min, indicating that the enamide is stable under physiological conditions. However, at pH 2, full conversion to the aldehyde was seen, verifying conversion of the enamide to the aldehyde following deacetylation, and highlighting the potential for use of enamides as an aldehyde protecting group in chemical synthesis.

Next, we determined whether deacetylation, the first step of activity-based HDAC detection by HP-1, could be effected by recombinant HDAC enzymes. Incubation of HP-1 with HDAC isoforms was performed with or without the potent HDAC inhibitor suberoylanilide hydroxamic acid (SAHA) to verify that any detected deacetylation was a result of enzymatic activity.[33,34] LC−MS analysis indicated good conversion of HP-1 to DHP-1 in the presence of both HDAC1 and 3 isoforms with a k_{obs} with HDAC3 of $3.2 \times 10^{-5} \pm 6 \times 10^{-6}$ s^{-1} and conversion $t_{1/2}$ of ~6 h. (Table 1, Supplementary Figure S2). By comparison, recombinant HDAC2, 6, and 8 as well as sirtuins 1 and 3 (HDAC Class III) did not deacetylate HP-1, giving HP-1 a distinct selectivity profile compared to activity-based probes designed around SAHA, a general Class I/II HDAC inhibitor.[31,32] While we recognized the need for ultimately optimizing the reaction rate through chemical modifications, we pressed on to assess the enamide in more biologically relevant contexts. Before proceeding we did, however, assess "off-target" selectivity. To further test the selectivity of HP-1 deacetylation, HP-1 was incubated with enzymes from three different protease classes (serine, cysteine, and aspartate). These proteases, which were confirmed as being active with positive control substrates, were also unable to convert HP-1 to DHP-1, further indicating selectivity of HP-1 for a subset of Class I HDAC enzymes (Table 1). Analyses of LC−MS traces from HP-1 deacetylation indicate that the *cis*-isomer of HP-1 is not deacetylated by HDAC1 or 3, suggesting

Table 1. Enzyme-Catalyzed Aldehyde Unmasking[a]

enzyme	% HP-1 to DHP-1[b]	
	− SAHA	+ SAHA
HDAC1	15	0
HDAC2	0	0
HDAC3	93	0
HDAC6	0	0
HDAC8	0	0
Sirtuin 1	0	N/A
Sirtuin 3	0	N/A
Chymotrypsin	0	N/A
Pepsin	0	N/A
Cathepsin B	0	N/A

[a]The unmasked aldehyde DHP-1 is produced by enzymatic deacetylation. Percent conversion of HP-1 to DHP-1 by HDAC and Sirtuin enzymes and various proteases. A mixture of *trans* and *cis* isomers (1.5:1) of HP-1 was used for all assays; HDAC enzymes cleave only the *trans* isomer. [b]Percentages indicate maximum detected conversion to DHP-1.

that *cis*-HP-1 does not bind to these isoforms or that the isoforms are unable to deacetylate *cis*-HP-1 (Supplementary Figure S2). Deacetylation of HP-2 was also afforded by HDAC1 and 3 but not by HDAC2, 6, or 8 (Supplementary Table S1), indicating that the presence of the double bond in *trans*-HP-1 does not significantly alter the HDAC isoform selectivity.

Competitive inhibition of HP-1 and -2 with a peptide substrate for HDAC isoforms was also examined to explore HDAC isoform selectivity. The measured IC$_{50}$ values indicate that some HDAC isoform selectivity may be related to binding affinity, as both HP-1 and -2 are deacetylated by and weakly inhibit HDAC1 (Table 2, Supplementary Figures S3 and S4).

Table 2. HP-1 Binds to Three HDAC Isoforms

isoform	IC$_{50}$ (μM)
HDAC1	35.8
HDAC2	>70
HDAC3	59
HDAC6	12
HDAC8	>70

However, both HP-1 and -2 are deacetylated by HDAC3, but only HP-1 has a detectable IC$_{50}$ for HDAC3. Furthermore, both HP-1 and -2 bind HDAC6, but neither were deacetylated by this isoform. Taken together, these data indicate that the selectivity of deacetylation of HP-1 and -2 is not dependent on binding affinity alone.

Following confirmation of HDAC-selective deacetylation of HP-1, we verified that deacetylated HP-1 could covalently interact with proteins (Figure 2a). Initially, HP-1 was incubated with HDAC3 to form DHP-1. We then added bovine serum albumin to induce formation of covalent protein-DHP-1 bonds
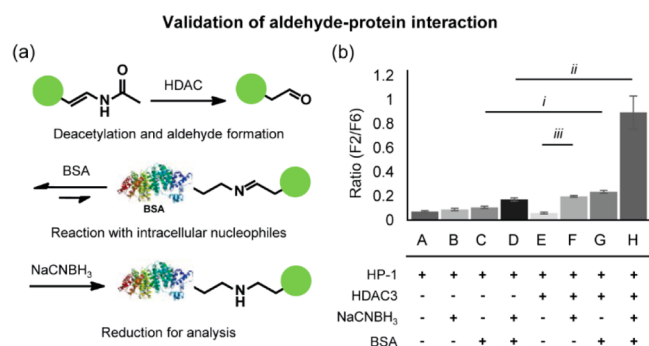
Figure 2. Unmasked aldehyde DHP-1 is produced by enzymatic deacetylation and forms conjugates with adventitious nucleophiles on proteins. (a) Mechanism of increased intracellular retention of HP-1 following conversion to DHP-1. (b) Ratio of fluorescence from the protein-DHP-1 conjugate (fraction 2) and unbound HP-1 and DHP-1 (fraction 6) collected during gel filtration chromatography of reactions A−H (A: HP-1; B: HP-1 and NaCNBH$_3$; C: HP-1 and BSA; D: HP-1, NaCNBH$_3$, and BSA; E: HP-1 and HDAC3; F: HP-1, HDAC3, and NaCNBH$_3$; G: HP-1, HDAC3, and BSA; H: HP-1, HDAC3, NaCNBH$_3$, and BSA). In the presence of BSA, DHP-1-protein conjugation occurs in the absence (i, $p < 0.001$) or presence (ii, $p < 0.001$) of NaCNBH$_3$. In the absence of BSA, HDAC3 deacetylates HP-1 and conjugates with DHP-1 in the presence of NaCNBH$_3$ (iii, $p < 0.001$). Statistical analyses were performed with a two-tailed Student's t test. A−H, $n = 3$ and error bars indicate ± SD.

(i.e., imines), which resulted in a 2-fold increase in detected protein-DHP-1 binding relative to controls (Figure 2b, lanes E and G, i; Supplementary Figure S5). We also tested conditions with sodium cyanoborohydride (NaCNBH$_3$) in order to accumulate the protein-DHP-1 conjugates via imine reduction (Figure 2a). These conditions showed a greater level of protein-DHP-1 binding, with a 5-fold increase compared to controls (Figure 2b, lanes F and H, ii; Supplementary Figure S5). This detection of the covalent interactions between DHP-1 and adventitious nucleophiles of proteins demonstrates the potential for the DHP-1 aldehyde functionality to retain the deacetylated probe within cells.

Initial examination of the HDAC-dependent deacetylation of HP-1 in a cellular context was carried out using HeLa whole-cell lysate and nuclear extract, as HeLa cells are known to have a high expression of HDACs.[35] HP-1 was converted to DHP-1 by both the whole-cell lysate and nuclear extract, and the production of DHP-1 was not detected following addition of the HDAC inhibitor SAHA (Supplementary Table S2). Following this, the deacetylation of HP-1 and -2 was analyzed in live HeLa cells via incubation with the probes over 24 h in the absence or presence of SAHA. Analysis of cell supernatants and lysates by LC−MS demonstrates that in the absence of SAHA 80% of HP-1 is cleaved over 24 h, forming a UV-active peak that we expect is DHP-1 bound to one or several cellular nucleophiles, although we have yet to specifically be able to identify these conjugates despite considerable effort. However, through separation of the lysate into protein-bound and unbound fractions it was determined that 33% of the intracellular fluorescent signal is attributable to the protein-bound probe (Figure 3a). Additionally, the percent of HP-1 found in the lysate (2%) does not change after incubation of the cells with SAHA for 24 h, indicating that HP-1 has reached and maintained an equilibrium between the intra- and extracellular space that is not altered by SAHA. Cleavage of HP-1 incubated with HeLa cells could be reduced to 20% over
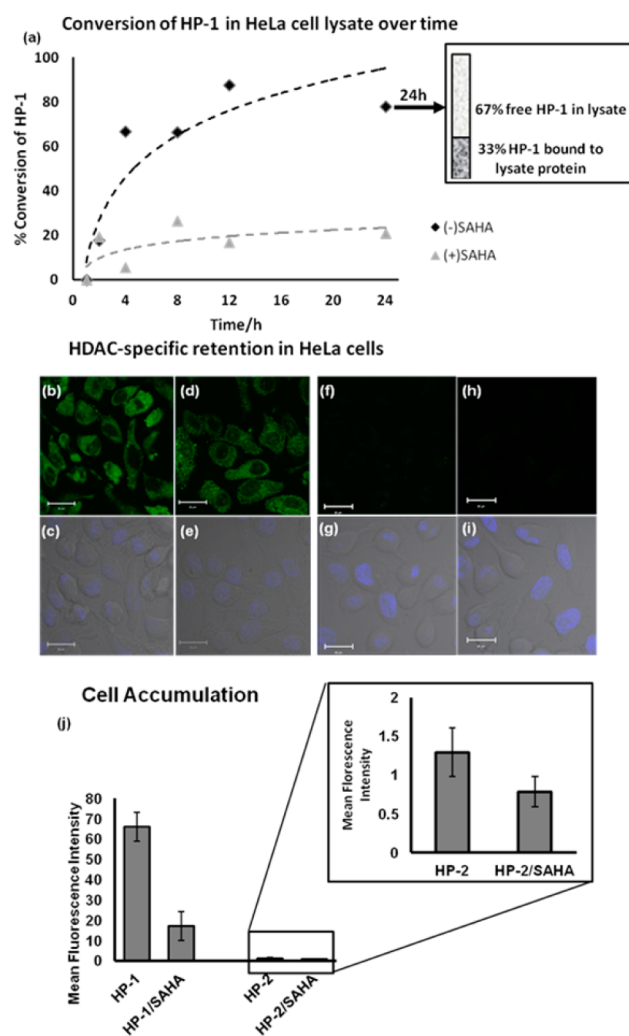

Figure 3. Cellular accumulation of enamide probe HP-1 is sensitive to HDAC activity. (a) Trapping of HP-1 in HeLa cell lysate. (b−e) Confocal microscopy images of HeLa cells in the absence (b, c) or presence (d, e) of 10 μM SAHA, added 15 min prior to incubation with 5 μM HP-1 for 2 h. Scale bars = 20 μm. (b, d) Intracellular NBD fluorescence. (c, e) DAPI nuclear stain with brightfield overlay. (f−i) Confocal microscopy images of HeLa cells in the absence (f, g) or presence (h, i) of 10 μM SAHA, added 15 min prior to incubation with 5 μM HP-2 for 2 h. Scale bars = 20 μm. (f, h) Intracellular NBD fluorescence. (g, i) DAPI nuclear stain with brightfield overlay. (e) Mean NBD fluorescence intensity of cells with 5 μM HP-1 or HP-2 ± 10 μM SAHA; $n = 9$, error bars indicate ± SD.

24 h through addition of SAHA (Figure 3a). By comparison, HP-2 incubated for 24 h with HeLa cells has a 7.8% conversion to DHP-2 in the absence of SAHA and no detectable conversion to DHP-2 when SAHA is added.

To examine the activity-based cellular retention of HP-1 and -2, the probes were incubated with HeLa cells for 2 h prior to confocal fluorescence imaging. Incubation was performed in the absence or presence of SAHA to probe the specificity of HP-1 retention for HDAC activity. As anticipated, HP-1 incubation in HeLa cells resulted in a robust intracellular fluorescent signal, while addition of SAHA reduces the level of fluorescence (Figure 3b−e,j), indicating that HP-1 deacetylation and cellular accumulation is sensitive to changes in HDAC activity. Interestingly, the HP-1 signal was localized to the cytoplasm, suggesting that HP-1 deacetylation occurred outside the

nucleus or that DHP-1 diffused out of the nucleus and accumulated in the cytoplasm via interaction with intracellular nucleophiles. It is worth noting that some HDACs are known to exist in the cytoplasm as multiprotein complexes.[36−38] When HP-2 is utilized for HeLa cell imaging, fluorescence was not detected within the HeLa cells either in the absence or presence of SAHA (Figure 3f−j), indicating that the trappable aldehyde released by HP-1 is essential for intracellular accumulation of the fluorescent NBD moiety and the detection of alterations in HDAC activity.

Taken together, our data indicate that HP-1 is a HDAC-selective fluorescent probe that contains a chemical moiety that confers increased intracellular retention following deacetylation by HDAC enzymes. We note some areas for improvement, including increasing the rate of deacetylation and improving selectivity for a single HDAC isoform, which may be accomplished through future structural modifications. It will also be critical moving forward to reduce the level of nonspecific accumulation, while increasing the overall uptake.

In summary, we have developed a novel probe for detection of HDAC activity that utilizes a unique aldehyde-trapping strategy for the accumulation of deacetylated HP-1 within cells. This accumulation results in increased fluorescence in cells with greater HDAC activity, thus affording a probe suitable for detection of HDAC activity via an activity-based cellular retention mechanism. When extrapolated to cells within an organism, this enamide-unmasking accumulation approach offers a mechanism for increased accumulation of the unmasked aldehyde and its attached cargo in cells and tissues with increased HDAC activity. Importantly, the cargo of the unmasked aldehyde can be easily adapted to contain tracers for positron emission tomography or contrast agents for magnetic resonance imaging, thus making the described enamide-accumulation approach a potential strategy for locating increased HDAC activity *in vivo*. Further, the aldehyde accumulation strategy could be modified to detect activity from other enzymes provided substrate catalysis can drive the unmasking of an aldehyde functional group.

■ METHODS

General Methods. All chemical reagents were of ACS grade purity or higher and used as received without further purification. Reactions were performed using standard techniques, including inert atmosphere of nitrogen with standard Schlenk technique, when necessary. Glassware was oven-dried at 150 °C overnight. Analytical thin layer chromatography (TLC) was performed on SiliCycle TLC silica Gel 60-F254 plates with visualization by ultraviolet (UV) irradiation at 254 nm. Purifications were performed using HP silica chromatography columns by Teledyne Isco. The elution system for each purification was determined by TLC analysis. Chromatography solvents were purchased from commercial sources and used without distillation. NMR spectra were recorded at 22 °C on a Varian 500 MHz spectrometer (^{1}H, 500.16 MHz and ^{13}C, 125.784 MHz). ^{1}H and ^{13}C NMR chemical shifts are reported as δ in units of parts per million (ppm) utilizing residual solvent signals for referencing. HPLC analysis of organic synthetic reactions was conducted on an Agilent 1100 series HPLC, and mass spectrometry data were recorded on an Agilent 6310 ion trap mass spectrometer (ESI source).

Synthesis of HP-1. HP-1 and -2 were synthesized in 7 and 2 synthetic steps, respectively. Detailed syntheses of HP-1 and -2 are reported in the Supporting Information.

LC−MS Characterization of HDAC Enzymatic Action on HP-1 and HP-2. The enzymatic cleavage of HP-1 and HP-2 was analyzed by LC−MS assays with HeLa nuclear extract (AnaSpec), HeLa whole cell lysate (Santa Cruz Inc.), and the purified HDAC isoforms: 1, 2, 3, 6,

and 8 (HDAC1, 3, and 8 from Cayman Chemicals and HDAC2, and 6 provided by Dr. Stephen Haggarty). Each sample in HDAC buffer was incubated for 12 h at 37 °C. Following incubation, an aliquot of supernatant from each sample was analyzed by LC−MS. Deacetylation of HP-1 and -2 was confirmed by detection of the $(M + H)^+$ ion following positive electrospray ionization. The peak area for each detected compound was measured to determine the % deacetylation of each probe. Full experimental details are in the Supporting Information.

LC−MS Analysis of HP-1 Cleavage by HDAC3 Enzyme over Time and Determination of the Observed Rate Constant (k_{obs}). The rate of cleavage of HP-1 by purified HDAC3 was analyzed by performing a LC−MS assay. Solutions containing HP-1 and HDAC3 in HDAC buffer were incubated for 12 h at 37 °C, and aliquots of supernatant from each sample were analyzed by LC−MS at t = 0, 1, 2, 4, 8, and 12 h. Deacetylation of HP-1 was confirmed by detection of the $(M + H)^+$ ion following positive electrospray ionization. The peak area for each detected compound was measured to determine the % deacetylation. The observed rate constant was determined using Graphpad by plotting Ln(DHP-1 peak area) versus time. Full experimental details are in the Supporting Information.

Characterization of Sirtuin (HDAC Class III) and Protease Enzymatic Action on HP-1. The enzymatic cleavage of HP-1 was analyzed by performing LC−MS assays with sirtuin 1 and 3 (Cayman Chemicals) and the proteases chymotrypsin (Sigma-Aldrich), cathepsin (EMD Millipore), and pepsin (Sigma-Aldrich). Full experimental details are in the Supporting Information.

IC$_{50}$ Measurements. HP-1 and HP-2 IC$_{50}$ values for HDAC1 were determined using the trypsin-coupled assay as well as the Caliper end point assay. HP-1 and HP-2 IC$_{50}$ values for HDAC2, HDAC3, HDAC6, and HDAC8 were determined with the Caliper end point assay. Full experimental details are in the Supporting Information.

HP-1 Deacetylation and Protein Binding Assay. Solutions containing HP-1 (20 μM) in 30 μL of HDAC buffer with 5% DMSO were incubated at 37 °C for 4 h in the presence or absence of HDAC3 (3.6 μM). After incubation with HDAC3, NaCNBH$_3$ (1.4 mM) or vehicle (H$_2$O) and BSA (6 mg mL^{-1}) or vehicle (HDAC buffer) were added to the solutions prior to an additional incubation at 37 °C for 2 h. Following the second incubation, the final samples were separated by G-25 columns (GE Healthcare), and the eluent was collected separately to obtain fractions 2−12. The fractions were transferred to a well in a 96-well, black, clear-bottom plate (Corning Incorporated), and the fluorescence was detected using an IVIS Spectrum (Caliper). To obtain the fluorescence signals, the 465 nm excitation filter, 530 nm emission filter, and a 5 s exposure were used. For analysis, the total photon flux over the area of each well was determined. Full experimental details are in the Supporting Information.

HDAC Activity in HeLa Cells with HP-1. *HeLa Cell Culture and Treatment with HP-1 and HP-2.* HeLa cells (ATCC) were grown as a monolayer in Eagles Minimum Essential Medium (EMEM, GIBCO, BRL) with 10% fetal bovine serum (FBS, GIBCO, BRL) and 1% penicillin/streptomycin (100 mg mL^{-1}). All cell culture dishes were maintained in a humidified atmosphere with 5% CO$_2$ at 37 °C.

Determination of HDAC Activity in HeLa Cells by LC−MS. HeLa cells grown in 600 mL cell culture flasks were treated with HP-1 or -2 ± SAHA so that the final concentrations were 5 μM for HP-1 and -2 and 10 μM for SAHA. Incubations were in HDAC buffer with 0.01% DMSO at 37 °C for t = 1, 2, 4, 8, 12, and 24 h. Following incubation, the medium was removed, and the cells were washed three times with DPBS buffer. Cells were scraped off of the flask and lysed in Millipore water using a mechanical homogenizer, and the supernatant of the lysed samples was analyzed by LC−MS. Cleavage and accumulation was confirmed by detection of the $(M + H)^+$ ion following positive electrospray ionization. The peak area for each detected compound was measured to determine the % conversion versus time. Full experimental details are in the Supporting Information.

Determination of HDAC Activity in HeLa Cells by Fluorescence. HeLa cells grown in 600 mL cell culture flasks were treated with HP-1 or -2 ± SAHA so that the final concentrations were 5 μM for HP-1 and -2 and 10 μM for SAHA. Incubations were in HDAC buffer with

0.01% DMSO) at 37 °C for t = 1, 2, 4, 8, 12 and 24 h. Following incubation, the medium was removed, and the cells were washed three times with DPBS buffer. Cells were scraped off of the flask and lysed in Millipore water using a mechanical homogenizer, and the protein bound probe fraction of cell lysate was separated by a Micron centrifugal filter device. Each cell lysate sample (before and after separation) was transferred to a well in a 96-well, black, clear-bottom plate (Corning Incorporated), and the fluorescence was detected using an IVIS Spectrum (Caliper). To obtain the fluorescence signals, a 465 nm excitation filter, a 530 nm emission filter, and a 1 s exposure were used. For analysis, the total photon flux over the area of each well was determined. Full experimental details are in the Supporting Information.

Imaging HDAC Activity in HeLa Cells with HP-1 and HP-2. An acid-washed, polylysine-treated sterile glass coverslip was added to each well of a 6-well plate, and HeLa cells were plated at a seeding density of ~2.5 × 10^5 cells mL^{-1} in 2 mL of growth medium. After 24 h, the cells reached 80−85% confluence. Cells were treated with HP-1, HP-1 with SAHA, HP-2, or HP-2 with SAHA so that the final concentrations of HP-1 and HP-2 were 5 μM in HDAC buffer (with 0.01% DMSO) and incubated at 37 °C for 2 h. Following incubation, the medium was removed, and the cells were washed three times with HDAC buffer and fixed with 4% paraformaldehyde in PBS. Coverslips were mounted on a drop of Gel Mount (antifade with DAPI nuclear stain) and analyzed by confocal imaging.

Confocal Fluorescence Imaging. Confocal fluorescence imaging was performed with a Zeiss laser scanning microscope 710 with a 63× objective lens and Zen 2009 software (Carl Zeiss). HP-1 and HP-2 were excited using a 488 nm Ar laser, and emission was collected using a META detector between 500 and 650 nm. Full imaging and analytical data are in the Supporting Informaqtion.

■ ASSOCIATED CONTENT

Ⓢ Supporting Information

This material is available free of charge via the Internet at http://pubs.acs.org.

■ AUTHOR INFORMATION

Corresponding Author
*E-mail: hooker@nmr.mgh.harvard.edu.

Notes
The authors declare no competing financial interest.

■ ACKNOWLEDGMENTS

■ REFERENCES

(1) Johnsson, N., and Johnsson, K. (2007) Chemical tools for biomolecular imaging. *ACS Chem. Biol. 2*, 31−38.
(2) Prescher, J. A., and Bertozzi, C. R. (2005) Chemistry in living systems. *Nat. Chem. Biol. 1*, 13−21.
(3) Kobayashi, H., Ogawa, M., Alford, R., Choyke, P. L., and Urano, Y. (2010) New strategies for fluorescent probe design in medical diagnostic imaging. *Chem. Rev. 110*, 2620−2640.
(4) Baruch, A., Jeffery, D. A., and Bogyo, M. (2004) Enzyme activity—it's all about image. *Trends Cell Biol. 14*, 29−35.
(5) Blum, G., Mullins, S. R., Keren, K., Fonovič, M., Jedeszko, C., Rice, M. J., Sloane, B. F., and Bogyo, M. (2005) Dynamic imaging of protease activity with fluorescently quenched activity-based probes. *Nat. Chem. Biol. 1*, 203−209.
(6) Weissleder, R., Tung, C.-H., Mahmood, U., and Bogdanov, A. (1999) In vivo imaging of tumors with protease-activated near-infrared fluorescent probes. *Nat. Biotechnol. 17*, 375−378.

(7) Wysocki, L. M., and Lavis, L. D. (2011) Advances in the chemistry of small molecule fluorescent probes. *Curr. Opin. Chem. Biol. 15* (6), 752−759.
(8) Tian, L., Yang, Y., Wysocki, L. M., Arnold, A. C., Hu, A., Ravichandran, B., Sternson, S. M., Looger, L. L., and Lavis, L. D. (2012) Selective esterase−ester pair for targeting small molecules with cellular specificity. *Proc. Natl. Acad. Sci. U.S.A. 109*, 4756−4761.
(9) Yeh, H.-H., Tian, M., Hinz, R., Young, D., Shavrin, A., Mukhapadhyay, U., Flores, L. G., Balatoni, J., Soghomonyan, S., and Jeong, H. J. (2012) Imaging epigenetic regulation by histone deacetylases in the brain using PET/MRI with 18 F-FAHA. *NeuroImage 64*, 630−639.
(10) Cheng, T.-C., Roffler, S. R., Tzou, S.-C., Chuang, K.-H., Su, Y.-C., Chuang, C.-H., Kao, C.-H., Chen, C.-S., Harn, I.-H., and Liu, K.-Y. (2012) An activity-based near-infrared glucuronide trapping probe for imaging β-glucuronidase expression in deep tissues. *J. Am. Chem. Soc. 134*, 3103−3110.
(11) Baba, R., Hori, Y., Mizukami, S., and Kikuchi, K. (2012) Development of a fluorogenic probe with a transesterification switch for detection of histone deacetylase activity. *J. Am. Chem. Soc. 134*, 14310−14313.
(12) Sasaki, K., Ito, A., and Yoshida, M. (2012) Development of live-cell imaging probes for monitoring histone modifications. *Bioorg.Med. Chem. 20*, 1887−1892.
(13) Coleman, R. E. (2000) FDG imaging. *Nucl. Med. Biol. 27*, 689−690.
(14) Ido, T., Wan, C., Fowler, J., and Wolf, A. (1977) Fluorination with molecular fluorine. A convenient synthesis of 2-deoxy-2-fluoro-D-glucose. *J. Org. Chem. 42*, 2341−2342.
(15) Hooker, J. M. (2010) Modular strategies for PET imaging agents. *Curr. Opin. Chem. Biol. 14*, 105−111.
(16) Roth, S. Y., Denu, J. M., and Allis, C. D. (2001) Histone acetyltransferases. *Annu. Rev. Biochem. 70*, 81−120.
(17) Allfrey, V., Faulkner, R., and Mirsky, A. (1964) Acetylation and methylation of histones and their possible role in the regulation of RNA synthesis. *Proc. Natl. Acad. Sci. U.S.A. 51*, 786.
(18) Balch, C., Fang, F., Matei, D. E., Huang, T. H.-M., and Nephew, K. P. (2009) Minireview: epigenetic changes in ovarian cancer. *Endocrinology 150*, 4003−4011.
(19) Strahl, B. D., and Allis, C. D. (2000) The language of covalent histone modifications. *Nature 403*, 41−45.
(20) Agalioti, T., Chen, G., and Thanos, D. (2002) Deciphering the transcriptional histone acetylation code for a human gene. *Cell 111*, 381−392.
(21) Ellis, L., Atadja, P. W., and Johnstone, R. W. (2009) Epigenetics in cancer: targeting chromatin modifications. *Mol. Cancer Ther. 8*, 1409−1420.
(22) Hendrich, B., and Bickmore, W. (2001) Human diseases with underlying defects in chromatin structure and modification. *Hum. Mol. Genet. 10*, 2233−2242.
(23) Kuo, M.-H., and Allis, C. D. (1998) Roles of histone acetyltransferases and deacetylases in gene regulation. *Bioessays 20*, 615−626.
(24) Minucci, S., and Pelicci, P. G. (2006) Histone deacetylase inhibitors and the promise of epigenetic (and more) treatments for cancer. *Nat. Rev. Cancer 6*, 38−51.
(25) Rodenhiser, D., and Mann, M. (2006) Epigenetics and human disease: translating basic biology into clinical applications. *Can. Med. Assoc. J. 174*, 341−348.
(26) Grayson, D. R., Kundakovic, M., and Sharma, R. P. (2010) Is there a future for histone deacetylase inhibitors in the pharmacotherapy of psychiatric disorders? *Mol. Pharmacol. 77*, 126−135.
(27) Gray, S. G. (2011) Epigenetic treatment of neurological disease. *Epigenomics 3*, 431−450.
(28) Butler, R., and Bates, G. P. (2006) Histone deacetylase inhibitors as therapeutics for polyglutamine disorders. *Nat. Rev. Neurosci. 7*, 784−796.

(29) Dietz, K. C., and Casaccia, P. (2010) HDAC inhibitors and neurodegeneration: at the edge between protection and damage. *Pharmacol. Res. 62*, 11−17.

(30) Sadri-Vakili, G., and Cha, J.-H. J. (2006) Histone deacetylase inhibitors: A novel therapeutic approach to Huntington's Disease (complex mechanism of neuronal death). *Curr. Alzheimer Res. 3*, 403−408.

(31) Salisbury, C. M., and Cravatt, B. F. (2007) Activity-based probes for proteomic profiling of histone deacetylase complexes. *Proc. Natl. Acad. Sci. U.S.A. 104*, 1171−1176.

(32) Salisbury, C. M., and Cravatt, B. F. (2008) Optimization of activity-based probes for proteomic profiling of histone deacetylase complexes. *J. Am. Chem. Soc. 130*, 2184−2194.

(33) Grant, S., Easley, C., and Kirkpatrick, P. (2007) Vorinostat. *Nat. Rev. Drug Discovery 6*, 21−22.

(34) Mann, B. S., Johnson, J. R., Cohen, M. H., Justice, R., and Pazdur, R. (2007) FDA approval summary: vorinostat for treatment of advanced primary cutaneous T-cell lymphoma. *Oncologist 12*, 1247−1252.

(35) Dueñas-González, A., Lizano, M., Candelaria, M., Cetina, L., Arce, C., and Cervera, E. (2005) Epigenetics of cervical cancer. An overview and therapeutic perspectives. *Mol. Cancer 4*, 38.

(36) Khochbin, S., Verdel, A., Lemercier, C., and Seigneurin-Berny, D. (2001) Functional significance of histone deacetylase diversity. *Curr. Opin. Genet. Dev. 11*, 162−166.

(37) Yang, W.-M., Tsai, S.-C., Wen, Y.-D., Fejér, G., and Seto, E. (2002) Functional domains of histone deacetylase-3. *J. Biol. Chem. 277*, 9447−9454.

(38) Fischle, W., Dequiedt, F., Hendzel, M. J., Guenther, M. G., Lazar, M. A., Voelter, W., and Verdin, E. (2002) Enzymatic activity associated with class II HDACs s dependent on a multiprotein complex containing HDAC3 and SMRT/N-CoR. *Mol. Cell 9*, 45−57.